Note

A structural investigation of the carbocation complex [{Cp*(CO)$_2$Fe}$_2${μ-(C$_3$H$_5$)}]PF$_6$

Evans O. Changamu [a], Holger B. Friedrich [a,*], R. Alan Howie [b], Melanie Rademeyer [c]

[a] *School of Chemistry, University of KwaZulu-Natal, Durban 4041, South Africa*
[b] *Department of Chemistry, University of Aberdeen, Meston Walk, Aberdeen AB24 3UE, Scotland, United Kingdom*
[c] *School of Chemistry, University of KwaZulu-Natal, Private Bag X01, Scottsville, Pietermaritzburg 3209, South Africa*

Abstract

The reaction of the propanediyl complex [{Cp*(CO)$_2$Fe}$_2${μ-(C$_3$H$_6$)}] (Cp* = η^5-C$_5$(CH$_3$)$_5$) with the hydride abstractor Ph$_3$CPF$_6$ in dry CH$_2$Cl$_2$ resulted in the formation of the carbocation complex [{Cp*(CO)$_2$Fe}$_2${μ-(C$_3$H$_5$)}]PF$_6$. The complex formed triclinic crystals in the space group $P\bar{1}$ with $Z = 1$. In the structure one metal is bonded in the η^2-fashion, forming a chiral metallacyclopropane structure with the carbocation, while the other is σ-bonded to the same carbocation ligand. However, NMR evidence indicates that the structure observed in the solid state is not preserved in solution because the metallacyclopropane ring opens up, giving a structure in which more positive charge is localized on the β-CH carbon and which could be fluxional.
© 2007 Elsevier B.V. All rights reserved.

Keywords: Transition-metal-stabilized carbocations; Metallacyclopropane; Fluxional

1. Introduction

Transition metal-stabilized carbocations were generally regarded as activated transition metal-olefin complexes [1–7]. In this respect, hydride abstraction is regarded as one of the methods for the synthesis of transition metal-olefin complexes [8]. Transition metal-olefin complexes continue to attract interest because of their significance as model compounds for transition metal-olefin intermediates in a wide range of catalytic reactions and their applications in stoichiometric organic synthesis [9]. Structural studies on such complexes are important in revealing the nature of bonding between the metals and the unsaturated hydrocarbons. However, reports of crystal structures involving alkanediyl carbocation complexes are very sparse [10–13]. The first structurally characterized alkanediyl carbocation complex was reported in the late 1970s by Laing et al. [10]. These authors reported the crystal structure of the carbocation complex [{Cp(CO)$_2$Fe}$_2${μ-(C$_3$H$_5$)}]PF$_6$, **I**, (Cp = η^5-C$_5$H$_5$) in which both Fe centres are σ-bonded to the α-CH$_2$ groups of the carbocation bridge and each is simultaneously weakly linked to the β-CH$^+$ carbon of the same carbocation bridge. In this respect, this complex cannot be regarded as an olefin complex. Before these, Raper and McDonald had reported the crystal structures of closely related, but not carbocationic, platinum allyl complexes [Pt(C$_3$H$_5$)(C$_5$H$_7$O$_2$)]$_2$ and [Pt(C$_3$H$_5$)Cl]$_4$ [14] in which the Pt–C bonds fall within the range 2.02–2.17 Å.

We recently reported the crystal structures of the mixed-ligand C$_3$ carbocation complexes [Cp*(CO)$_2$Fe{μ-(C$_3$H$_5$)}Fe(CO)$_2$Cp]PF$_6$, **II**, (Cp* = η^5-C$_5$(CH$_3$)$_5$, Cp = η^5 -C$_5$H$_5$) [12] and [Cp*(CO)$_2$Fe{μ-(C$_3$H$_5$)}Ru(CO)$_2$Cp]PF$_6$ [13], which showed that the Fe attached to the Cp* ligand forms a chiral metallacyclopropane structure with the carbocation bridge, while the other metal centre is σ-bonded to the same carbocation bridge. Very recently we also reported the synthesis and NMR studies of the carbocation complexes [Cp*(CO)$_2$Fe{μ-(C$_n$H$_{2n-1}$)}M(CO)$_x$Cp]PF$_6$ (n = 3-6, x = 2, M = Fe or Ru; x = 3, M = W), [Cp(CO)$_2$Ru

---
* Corresponding author. Tel.: +27 31 2603107; fax: +27 31 2603109.
E-mail address: friedric@ukzn.ac.za (H.B. Friedrich).

{μ-(C$_n$H$_{2n-1}$)}W(CO)$_3$Cp]PF$_6$ (*n* = 3–5) [15], [{Cp(CO)$_2$-Fe}$_2${μ-(C$_2$H$_{2n-1}$)}]PF$_6$ (*n* = 4–10) and [{Cp(CO)$_2$Fe}$_2${μ-(C$_2$H$_{2n-2}$)}](PF$_6$)$_2$ (*n* = 5–10) [16]. The NMR evidence indicates that one metal in the monocationic complexes forms a chiral metallacyclopropane structure with the carbocation ligand and that this structure is preserved in solution. The positive charge appears to be delocalized within the metallacyclopropane ring. In the dicationic complexes, both metals form chiral metallacyclopropane type structures. The determination of the molecular structure of the complex [{Cp*(CO)$_2$Fe}$_2${μ-(C$_3$H$_5$)}]PF$_6$ is interesting, not only because it completes the structural studies on this series of the C$_3$ carbocation bridged complexes, but also because it reveals the influence of the bulky electron-releasing Cp* ligand on the type of crystal lattice adopted by the complexes.

2. Results and discussion

2.1. Synthesis of [{Cp*(CO)$_2$Fe}$_2${μ-(C$_3$H$_5$)}]PF$_6$

The overnight reaction of the neutral complex [{Cp*(CO)$_2$Fe}$_2${μ-(C$_3$H$_6$)}] with 1 equiv. of the hydride abstractor Ph$_3$CPF$_6$ gave a deep orange solution from which the orange solid [{Cp*(CO)$_2$Fe}$_2${μ-(C$_3$H$_5$)}]PF$_6$, **III**, was precipitated with diethyl ether. It is virtually insoluble in hydrocarbon solvents like hexane, but dissolves well in CH$_2$Cl$_2$, acetone, and dimethylformamide. It is stable in air in the solid state for several hours, but decomposes in N$_2$-saturated solutions after several days if kept in the dark, otherwise it decomposes in less than 2 h. The decomposition is rapid in solutions made from solvents that are not nitrogen-saturated.

2.2. NMR spectroscopy

The ^{1}H NMR spectrum observed is characteristic of an A$_4$X spin system. Thus, the spectrum shows one unsymmetrical doublet at 2.16 ppm (*J* = 10.1 Hz) due to the four α-CH$_2$ protons, a symmetrical quintet at 5.51 ppm due to the β-CH$^{\delta+}$ proton, and a singlet at 1.89 ppm due to the 30 protons of the Cp* ligands. Thus, the metallacyclopropane structure (Fig. 1a) observed in the solid state (Section 2.3) is not preserved in solution. The room temperature ^{13}C NMR spectrum shows only one signal due to the two α-CH$_2$ carbon atoms at 32 ppm. This may be considered as an average of the 45 ppm and 15 ppm expected for a rigid metallacyclopropane-containing structure and is more deshielded than the 24 ppm displayed by the corresponding CH$_2$ carbons of the symmetrical complex [{Cp(CO)$_2$Fe}$_2${μ-(C$_3$H$_5$)}]PF$_6$ [10]. This increased deshielding is unexpected given the fact that, in the complex [{Cp*(CO)$_2$Fe}$_2${μ-(C$_3$H$_5$)}]PF$_6$, the CH$_2$ carbons are α to metals attached to the electron-releasing Cp* ligand. It is, however, less deshielded than the 45 ppm displayed by the corresponding CH$_2$ carbon of the mixed–ligand complex [Cp*(CO)$_2$Fe{μ-(C$_3$H$_5$)}Fe(CO)$_2$Cp]PF$_6$ [15]. NMR data of the mixed-ligand complex showed that the structure is rigid even in solution with the metal attached to the Cp* ligand forming a metallacyclopropane structure with the carbocation ligand and the positive charge delocalised mainly within the metallacycle [15].

The β-CH$^+$ carbon signal at 124 ppm is more deshielded than the 118 ppm displayed by the corresponding carbon atom of the mixed-ligand complex [Cp*(CO)$_2$Fe{μ-(C$_3$H$_5$)}Fe(CO)$_2$Cp]PF$_6$, **II** [15]. This also indicates that there is more positive charge on the β-CH$^+$ of **III**, than on the α-CH$_2$ carbons, as also found for the symmetrical complex [{Cp(CO)$_2$Fe}$_2${μ-(C$_3$H$_5$)}]PF$_6$, **I** [10]. This implies that in solution, the nature of bonding between the metal centres and the carbocation in [{Cp*(CO)$_2$Fe}$_2${μ-(C$_3$H$_5$)}]PF$_6$ lies somewhere between the two extremes represented by the complexes [{Cp(CO)$_2$Fe}$_2${μ-(C$_3$H$_5$)}]PF$_6$, **I**, and [Cp*(CO)$_2$Fe{μ-(C$_3$H$_5$)}Fe(CO)$_2$Cp]PF$_6$, **II**. The signal due to the 5 equiv. C$_5$(CH$_3$)$_5$ ring carbon atoms at 98.7 ppm in compound **III** is less deshielded than the 100.2 ppm displayed by the corresponding ring carbon atoms of compound **II**.

The molecule may also be considered to be fluxional and the equilibria existing in solution may be presented as shown in Fig. 1. The solution NMR spectra observed are consistent with the species shown in Fig. 1b in which both of the α-CH$_2$ carbon atoms are equivalent and less deshielded than the metallacyclic α-CH$_2$ carbon of the structures shown in Fig. 1a and c, but more deshielded than the non-metallacyclic α-CH$_2$ carbon atoms of the structures shown in Fig. 1a and c.

The low temperature ^{1}H NMR spectrum (−50 °C) showed that the doublet at 2.16 ppm resolves into a multiplet, suggesting that some dynamic process is being frozen out. Above room temperature the ^{1}H NMR spectrum in DMF-*d$_7$* showed that the unsymmetrical doublet becomes symmetrical and remains unchanged until 100 °C, when the compound decomposes.

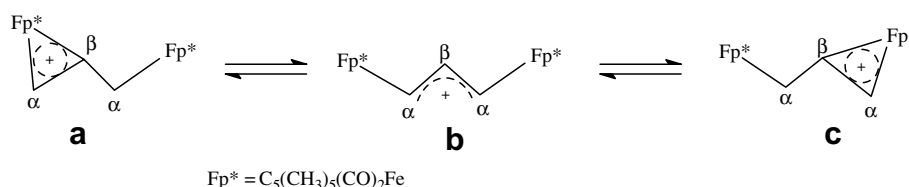Fig. 1. Dynamic equilibrium forms of the carbocation complex [{Cp*(CO)$_2$Fe}$_2${μ-(C$_3$H$_5$)}]PF$_6$.

2.3. X-ray crystallography

The complex $[\{Cp^*(CO)_2Fe\}_2\{\mu\text{-}(C_3H_5)\}]PF_6$ formed triclinic crystals in the space group $P\bar{1}$ with $Z = 1$. A suitable crystal was selected and subjected to X-ray diffraction studies.

The molecular structure of $[\{Cp^*(CO)_2Fe\}_2\{\mu\text{-}(C_3H_5)\}]PF_6$ (Fig. 2) shows the C14 of the alkanediyl carbocation disordered over two positions. Accordingly, the alkanediyl carbocation appears to be a C4 hydrocarbon, but in reality it is a C3 hydrocarbon. Because the molecule is symmetrical and only one metal can form a metallacyclopropane structure with the $\beta\text{-}CH^+$ carbon at a time (for steric reasons), there are two possible arrangements of the metal atoms in the structure. Therefore, at first sight the appearance of a C4 carbocation in the structure could simply be interpreted in terms of the disorder arising from the random distribution of the two possible arrangements (Fig. 3a and b) throughout the sample crystal. However, the C14–C13 and C13–C13^i^ bond distances of 1.135(6) Å and 1.479(7) Å, where the first is shorter than even a C–C triple bond and the latter comparable with an aromatic bond, suggest that simple disorder cannot fully explain the observed structure. In the light of the NMR results (discussed above), it seems reasonable to invoke fluxionality as a factor in the explanation of the observed structure.

Fig. 3 shows the two components, (a) and (b), of the disordered arrangement of the C_3H_5 bridge which creates the four sites observed in the crystal structure. Their superposition will produce the appearance of a four-carbon chain. In this model C14, H14a and H14b all have occupancy of 0.5. While C13 has full occupancy, the H atoms attached to it (now three in number) also have occupancies of 0.5. This creates the desired C_3H_5 formulation of the bridging

species. A careful application of the AFIX and PART instructions of SHELXL97 [17] allows the placement of the H atoms in calculated positions as required for the disordered model. Note that when a C13 atom is directly bonded to a C14 atom it is also bonded to H13a and NOT to H13b or H13c. On the other hand, when a C13 atom is bonded only to Fe and is behaving as a methylene C atom, it is also bonded to H13b and H13c, but NOT to H13a. The transition of 3(a) to 3(b) can be perceived as a sideways movement of the chain C14(methylene) to C13(methylene), C13(tertiary C) to C13^i^(tertiary C) and C13^i^(methylene) to C14^i^(methylene). Thus this model could be considered to be compatible with or indicative of fluctionality of the bridging species.

Selected bond angles and bond lengths are summarized in Table 1, while the data collection and reduction information is given in Table 2. The bond length of Fe–C_α = 2.195(4) Å is slightly longer than the 2.167(5) Å and 2.173(2) Å observed in the mixed ligand complexes $[Cp^*(CO)_2Fe\{\mu\text{-}(C_3H_5)\}Fe(CO)_2Cp]PF_6$ [12] and $[Cp^*(CO)_2Fe\{\mu\text{-}(C_3H_5)\}Ru(CO)_2Cp]PF_6$ [13]. It is, however, comparable to the 2.12 and 2.13 Å reported for the corresponding bond in $[\{Cp(CO)_2Fe\}_2\{\mu\text{-}(C_3H_5)\}]PF_6$ [10]. The bond length of Fe–C_β = 2.215(3) Å is shorter than the 2.302(6) Å [12] and 2.291(3) Å [13] observed in the mixed-ligand complexes, respectively. It is significantly shorter than the 2.59 and 2.72 Å reported for corresponding bonds in $[\{Cp(CO)_2Fe\}_2\{\mu\text{-}(C_3H_5)\}]PF_6$ [10]. The differences in the Fe–C_β and Fe–C_α bonds, relative to the corresponding bonds in the mixed-ligand complexes, may be due to the disorder in the complex $[\{Cp^*(CO)_2Fe\}_2\{\mu\text{-}(C_3H_5)\}]PF_6$. The bonds are longer than expected for a single Fe–C bond {2.069(10) Å [18] and 2.057(3) Å [19]}.

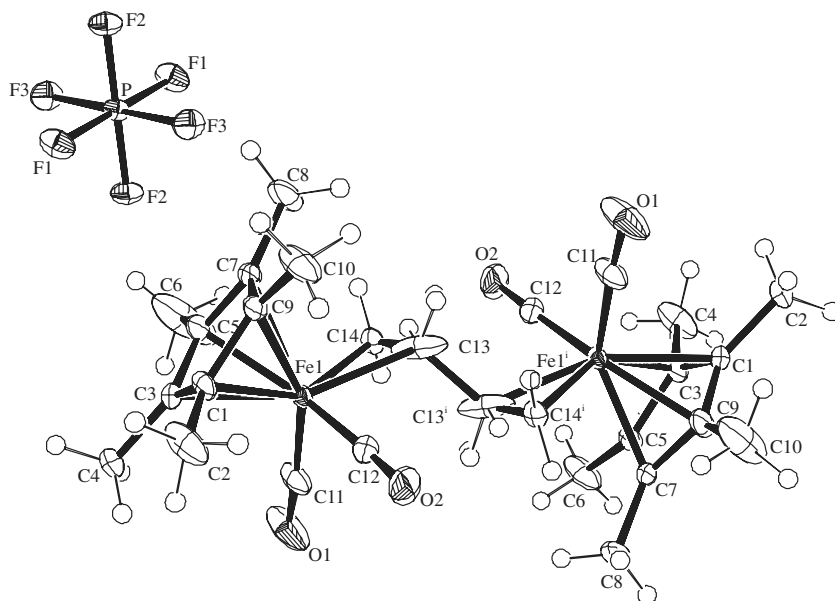Fig. 4 shows the molecular structures of the complexes $[\{Cp(CO)_2Fe\}_2\{\mu\text{-}(C_3H_5)\}]PF_6$, **I**, [10] $[Cp^*(CO)_2Fe$

Fig. 2. Perspective view of the molecular structure of $[\{Cp^*(CO)_2Fe\}_2\{\mu\text{-}(C_3H_5)\}]PF_6$. Thermal ellipsoids are drawn at 50% probability level.
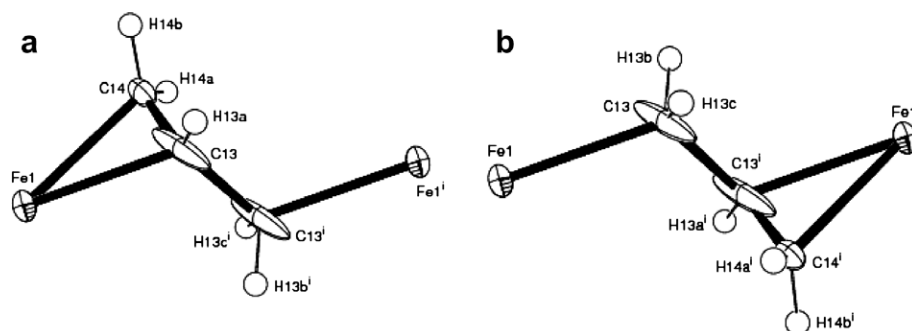
Fig. 3. Components of the disorder in the C_3H_5 bridge of the complex $[\{Cp^*(CO)_2Fe\}_2\{\mu-(C_3H_5)\}]PF_6$ Symmetry code (i) $-x$, $1-y$, $1-z$.

Table 1
Selected bond lengths and angles for $[\{Cp^*(CO)_2Fe\}_2\{\mu-(C_3H_5)\}]PF_6$

Bond lengths (Å)

Fe1–C12	1.764(3)	Fe1–C14	2.195(4)	C5–C7	1.405(4)
Fe1–C11	1.770(3)	Fe1–C13	2.215(3)	C5–C6	1.507(4)
Fe1–C3	2.093(2)	O1–C11	1.141(3)	C7–C9	1.432(4)
Fe1–C9	2.103(3)	O2–C12	1.150(3)	C7–C8	1.495(3)
Fe1–C1	2.104(2)	C1–C3	1.414(4)	C9–C10	1.492(4)
Fe1–C5	2.107(2)	C1–C9	1.434(3)	P–F1	1.6048(15)
Fe1–C7	2.138(2)	C1–C2	1.503(3)	P–F2	1.6075(15)
C14–C13	1.135(6)	C3–C5	1.451(3)	P–F3	1.6042(15)
C13–C13	1.479(7)	C3–C4	1.502(4)		

Bond angles (°)

C12–Fe1–C11	95.86(14)	C12–Fe1–C14	112.80(14)	C1–C3–Fe1	70.74(14)
C12–Fe1–C3	89.38(12)	C11–Fe1–C14	84.11(15)	C5–C3–Fe1	70.32(13)
C11–Fe1–C3	116.92(10)	C3–Fe1–C14	148.47(14)	C4–C3–Fe1	126.8(2)
C12–Fe1–C9	155.60(12)	C9–Fe1–C14	88.27(15)	C7–C5–C3	108.1(2)
C11–Fe1–C9	98.54(13)	C1–Fe1–C14	125.90(14)	C7–C5–C6	125.7(2)
C3–Fe1–C9	66.54(12)	C5–Fe1–C14	113.01(14)	C3–C5–C6	125.9(2)
C12–Fe1–C1	121.28(11)	C7–Fe1–C14	82.25(15)	C7–C5–Fe1	71.85(15)
C11–Fe1–C1	89.21(11)	C12–Fe1–C13	84.78(13)	C3–C5–Fe1	69.25(13)
C3–Fe1–C1	39.38(10)	C11–Fe1–C13	96.95(12)	C6–C5–Fe1	128.94(19)
C9–Fe1–C1	39.85(10)	C3–Fe1–C13	146.06(11)	C5–C7–C9	108.1(2)
C12–Fe1–C5	93.31(12)	C9–Fe1–C13	112.72(12)	C5–C7–C8	125.0(3)
C11–Fe1–C5	155.51(10)	C1–Fe1–C13	152.57(12)	C9–C7–C8	126.8(3)
C3–Fe1–C5	40.43(9)	C5–Fe1–C13	106.48(10)	C5–C7–Fe1	69.51(14)
C9–Fe1–C5	66.10(11)	C7–Fe1–C13	91.52(10)	C9–C7–Fe1	68.95(15)
C1–Fe1–C5	66.68(10)	C14–Fe1–C13	29.81(15)	C8–C7–Fe1	129.9(2)
C12–Fe1–C7	128.09(12)	C3–C1–Fe1	69.88(13)	C7–C9–C1	108.1(2)
C11–Fe1–C7	135.87(13)	C9–C1–Fe1	70.02(14)	C7–C9–C10	125.7(2)
C3–Fe1–C7	66.27(11)	C2–C1–Fe1	128.91(17)	F1–P–F1	180.0
C9–Fe1–C7	39.45(10)	C1–C3–C5	107.8(2)	F3–P–F2	90.32(8)
C1–Fe1–C7	66.31(9)	C1–C3–C4	126.4(2)	F1–P–F2	90.32(8)
C5–Fe1–C7	38.64(11)	C5–C3–C4	125.8(2)	F1–P–F2	89.68(8)
C10–C9–Fe1	128.2(3)	C7–C9–Fe1	71.60(14)	F2–P–F2	180.00
O2–C12–Fe1	175.8(2)	C1–C9–Fe1	70.13(13)	F3–P–F3	180.00
O1–C11–Fe1	176.4(3)	C1–C9–C10	125.9(2)	F3–P–F1	90.16(9)
C13–C14–Fe1	76.(3)	C3–C1–C9	107.8(2)	F3–P–F1	89.84(9)
C14–C13–C13	123.2(5)	C3–C1–C2	125.3(2)	F3–P–F2	89.68(8)
C14–C13–Fe1	74.1(3)	C9–C1–C2	126.8(2)		
C13–C13–Fe1	114.8(2)				

$\{\mu-(C_3H_5)\}Fe(CO)_2Cp]PF_6$, **II** [12] and $[\{Cp^*(CO)_2Fe\}_2-\{\mu-(C_3H_5)\}]PF_6$, **III**. Compounds **I** and **II** formed monoclinic crystals in the space groups $P2_1/n$ and Cc, respectively, while compound **III** formed triclinic crystals in the space group $P\bar{1}$. Compound **III** may be regarded as obtained from compound **I** by successive substitution of the Cp ligands with Cp^* ligands. In this respect, substitution of one Cp ligand gives complex **II** in which the Fe attached to the Cp^* ligand shows strong interaction with the β-$CH^{\delta+}$ group, unlike complex **I** in which both metal centres have weak interactions with the β-$CH^{\delta+}$ group. The geometry of the molecule is distorted to allow this

Table 2
Crystal data collection and experimental details for [{Cp*(CO)$_2$Fe}$_2$μ–(C$_3$H$_5$)]PF$_6$

Compound	[{Cp*(CO)$_2$Fe}$_2$(C$_3$H$_5$)]PF$_6$
Empirical formula	C$_{27}$H$_{35}$Fe$_2$F$_6$O$_4$P
Formula weight	680.23 g/mol
Crystal data	
Crystal system	Triclinic
Space group	$P\bar{1}$
Unit cell dimensions	
$a = 8.122(4)$ Å	$V = 713.5(5)$ Å^3
$b = 8.560(2)$ Å	$Z = 1$
$c = 11.554(3)$ Å	$D_x = 1.581$ Mg m^{-3}
$\alpha = 110.10(3)°$	$\mu = 1.144$ mm^{-1}
$\beta = 106.88(3)°$	$\theta = 5.03–31.88$
$\gamma = 92.08(3)°$	$T = 100(2)$ K
Crystal description	Block
Crystal colour	Brown
Crystal size (mm)	$0.2 \times 0.15 \times 0.15$
Data collection	
Oxford Excalibur 2 diffractometer	
$\omega - 2\theta$ scans	$h = -8 \rightarrow 11$
MoKα radiation	$k = -12 \rightarrow 12$
$F(000) = 350$	$l = -16 \rightarrow 17$
Refinement	
Reflections for cell parameters	1726
Transmission factors (T_{min}; T_{max})	0.8049; 0.8482
Measured reflections	7404
Independent reflections	4379
Observed reflections with $I > 2\sigma(I)$;	3522
$R_{int} = 0.0267$	$R_1 = 0.04553$
Final R indices [$F^2 > 2\sigma(F^2)$]	$wR(F^2) = 0.1247$
Goodness of fit on $F^2(S)$	1.085
192 Parameters	
Maximum shift	$(\Delta/\sigma)_{max} = 0.000$
Largest difference peak	$\Delta\rho_{max} = 0.925$ e A^{-3}
Largest hole	$\Delta\rho_{min} = -1.216$ e A^{-3}

Fig. 4. The influence of Cp* ligand on the structures of the complexes [{Cp(CO)$_2$Fe}$_2${μ-(C$_3$H$_5$)}]PF$_6$, I [10], [Cp*(CO)$_2$Fe{μ-(C$_3$H$_5$)}Fe(CO)$_2$Cp]PF$_6$, II, and [{Cp*(CO)$_2$Fe}$_2${μ-(C$_3$H$_5$)}]PF$_6$, III.

interaction and to reduce steric interaction between the bulky Cp* and the Cp ligands. Substitution of a second Cp with a Cp* ligand leads to the symmetrical compound III, which has similar bonding to that in compound II, but the spatial arrangement is such that the headgroups of the Cp* ligands face the top and bottom sides of the alkanediyl carbocation plane, respectively.

3. Conclusions

In the solid state one of the Fe metals in the complex [{Cp*(CO)$_2$Fe}$_2${μ-(C$_3$H$_5$)}]PF$_6$ forms a metallacyclopropane type structure with the carbocation bridge, while the other is σ-bonded. NMR evidence indicates that the metallacycopropane type structure observed in the solid state is not preserved in solution. The compound appears fluxional in solution, giving an average structure of a transition metal-stabilized carbenium ion. Thus, the complex [{Cp*(CO)$_2$Fe}$_2${μ-(C$_3$H$_5$)}]PF$_6$ behaves like the mixed-ligand complex [Cp*(CO)$_2$Fe{μ-(C$_3$H$_5$)}Fe(CO)$_2$Cp]PF$_6$ with respect to the formation of a chiral metallacyclopropane structure in the solid state. On the other hand, in solution it behaves like t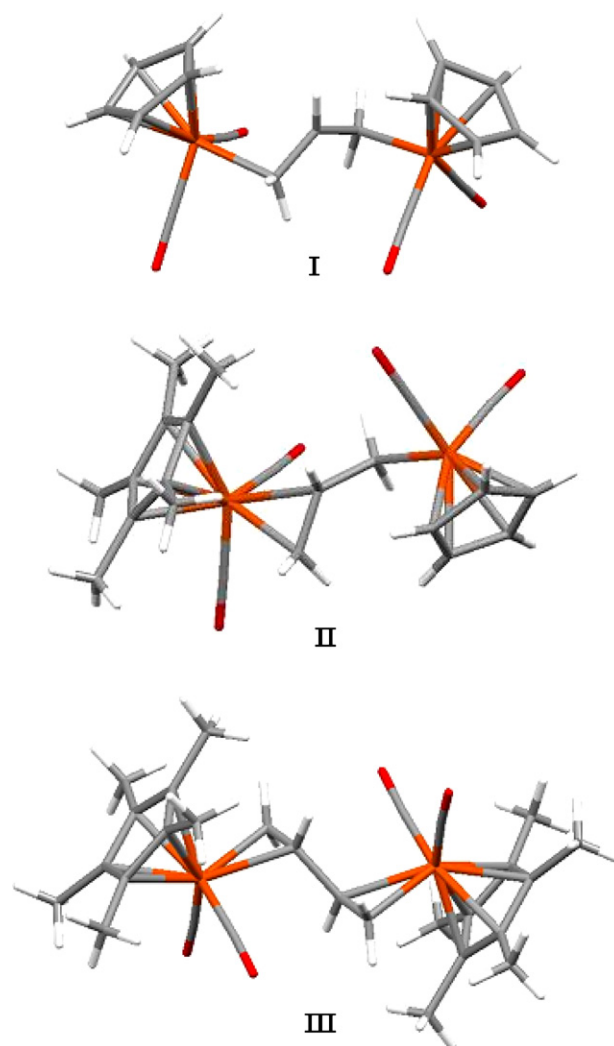he complex [{Cp(CO)$_2$Fe}$_2${μ-(C$_3$H$_5$)}]PF$_6$ which exists as a transition metal-stabilized carbenium ion both in the solid state and in solution.

4. Experimental

4.1. Synthesis of [{Cp*(CO)$_2$Fe}$_2${μ-(C$_3$H$_5$)}]PF$_6$

A filtered solution of Ph$_3$CPF$_6$ (0.99 g, 0.254 mmol) in CH$_2$Cl$_2$ (8 mL) was added to a solution of [{Cp*(CO)$_2$Fe}$_2${μ-(C$_3$H$_6$)}] [20] (0.136 g, 0.254 mmol) in CH$_2$Cl$_2$ (8 mL) in a Schlenk tube and the mixture allowed to stand overnight under nitrogen at room temperature. The resultant deep orange solution was filtered through a cannula into a pre-weighed Schlenk tube. Dry nitrogen-saturated diethyl ether was added to the solution and an orange microcrystalline solid precipitated. The mother liquor was syringed off and the solid dried under reduced pressure. Yield: 60%, Decomposed >140 °C. Anal. Calc. for C$_{27}$H$_{35}$F$_6$Fe$_2$O$_4$P:

C, 47.67; H, 5.19. Found: C, 47.31; H, 4.90%. IR (CH_2Cl_2, cm^{-1}): $v(CO)$, 2054, 2038, 1998, 1942. ^1H NMR (acetone-d_6, ppm): [δ] 1.89 (s, 30H, $C_5(CH_3)_5$), 2.16 (d, 4H, $J_{HH} = 10.1$ Hz, CH_2), 5.51 (q, 1H, CH). ^{13}C NMR (acetone-d_6, ppm): [δ] 9.4 ($C_5(CH_3)_5$), 32.2 (CH_2), 98.7 ($C_5(CH_3)_5$), 124.4 (CH).

4.2. X-ray crystallography

Crystals of [{Cp*(CO)$_2$Fe}$_2${μ-(C$_3$H$_5$)}]PF$_6$ suitable for X-ray diffraction studies were obtained by slow diffusion of a fivefold excess diethyl ether into a concentrated solution of the compound in acetone held at 278 K over a period of one week. X-ray diffraction intensity data were collected with an Oxford Excalibur 2 diffractometer (CrysAlis CCD 170) using Mo Kα radiation ($\lambda = 0.71073$ Å) with a $\omega - 2\theta$ scan mode [21] at 100(2) K. The structure was solved by direct methods using SHELXS97 and refined using SHELXL97 [17]. Data collection and reduction information are contained in Table 2.

Acknowledgements

Appendix A. Supplementary material

CCDC 648797 contains the supplementary crystallographic data for this paper. These data can be obtained free of charge via http://www.ccdc.cam.ac.uk/conts/retrieving.html, or from the Cambridge Crystallographic Data Centre, 12 Union Road, Cambridge CB2 1EZ, UK; fax: +44 1223 336 033; or e-mail: deposit@ccdc.cam.ac.uk. Supplementary data associated with this article can be found, in the online version, at doi:10.1016/j.jorganchem.2007.07.030.

References

[1] H.S. Clayton, J.R. Moss, M.E. Dry, J. Organomet. Chem. 688 (2003) 181–191.
[2] M. Cousins, M.L.H. Green, J. Chem. Soc. (1963) 889–894.
[3] W.P. Giering, M. Rosenblum, Chem. Commun. (1971) 441–442, and references therein.
[4] W.P. Giering, M. Rosenblum, J. Tancrede, J. Am. Chem. Soc. 94 (1972) 7170–7172.
[5] M.L.H. Green, P.L.I. Nagy, J. Am. Chem. Soc. 84 (1962) 1310.
[6] M.L.H. Green, P.L.I. Nagy, J. Chem. Soc. (1963) 189–197.
[7] M.L.H. Green, P.L.I. Nagy, J. Organomet. Chem. 1 (1963) 58–69.
[8] Ch. Elschenbroich, A. Salzer, Organometallics, A Concise Introduction, second revised ed., VCH, Weinheim, 1992 (Chapter 15).
[9] S.G. Davies, Organotransition Metal Chemistry: Applications to Organic Synthesis, Pergamon Press, Oxford, 1982.
[10] M. Laing, J.R. Moss, J. Johnson, J. Chem. Soc., Chem. Commun. (1977) 656–657.
[11] H.-J. Müller, U. Nagel, W. Beck, Organometallics 6 (1987) 193–194.
[12] E.O. Changamu, H.B. Friedrich, M. Rademeyer, Acta Crystallogr. E62 (2006) m442–m444.
[13] H.B. Friedrich, E.O. Changamu, M. Rademeyer, Acta Crystallogr. E62 (2006) m405–m407.
[14] G. Raper, W.S. McDonald, J. Chem. Soc., Dalton Trans. (1972) 265–269.
[15] E.O. Changamu, H.B. Friedrich, M. Rademeyer, J. Organomet. Chem. 692 (2007) 2456–2472.
[16] E.O. Changamu, H.B. Friedrich, J. Organomet. Chem. 692 (2007) 1138–1149.
[17] G.M. Sheldrick, SHELXS97 and SHELXL97, University of Göttingen, Germany, 1997.
[18] R.O. Hill, C.F. Marais, J.R. Moss, K.J. Naidoo, J. Organomet. Chem. 587 (1999) 28–37.
[19] H.B. Friedrich, M.O. Onani, M. Rademeyer, Acta Crystallogr. E60 (2004) m551–m553.
[20] S.F. Mapolie, J.R. Moss, S. Afr. J. Chem. 40 (1987) 12–16.
[21] Oxford Diffraction (2003). CrysAlis CCD and CrysAlis RED. Versions 1.170. Oxford Diffraction Ltd., Abingdon, Oxfordshire, England.